IRRIGATION AND DRAINAGE
Irrig. and Drain. **(2019)**
Published online in Wiley Online Library (wileyonlinelibrary.com) **DOI**: 10.1002/ird.2342

GENERAL EQUATION FOR ADVANCE AND RECESSION OF WATER IN BORDER IRRIGATION†

MOHAMMAD MAHDI CHARI[1]*, KAMRAN DAVARY[2], BIJAN GHAHRAMAN[2] AND ALI NAGHI ZIAEI[2]

[1] *Water Engineering Department, Faculty of Soil and Water, University of Zabol, Zabol, Iran*
[2] *Water Engineering Department, Faculty of Agriculture, Ferdowsi University of Mashhad, Mashhad, Iran*

ABSTRACT

Advance and recession curves are of great importance for assessing the performance of border irrigation. In recent years, scaling techniques have helped to reduce the required measurements and to provide formulation of soil–water relations. The purpose of this study was to develop an invariant equation for calculating advance and recession curves in border irrigation using scaling techniques. The kinematic wave model and the Philip infiltration equation were used to simulate border irrigation. Scale factors were defined such that the kinematic wave equation remained independent of the initial and boundary conditions of the soil. Scaled advance and recession curves showed certain patterns, which led us to introduce a power and a binomial equation for advance and recession phases, respectively. The scaled equations were applied on 25 vegetated and non-vegetated borders. Four performance indices were calculated for each border, including application efficiency (E_a), deep percolation ratio (DPR), tail water ratio (TWR) and water requirement efficiency (E_r). Results showed that the maximum differences between measured and estimated values were 4% for E_a, 9% for DPR and 4% for E_r. Considering the simplicity and soil-condition independence of the proposed method, it can be concluded that scaled advance and recession curves could provide a reasonable estimate of border irrigation performance. © 2019 John Wiley & Sons, Ltd.

KEY WORDS: border irrigation; infiltration; invariant solution; scaling

Received 13 May 2018; Revised 3 March 2019; Accepted 4 March 2019

RÉSUMÉ

Les courbes de progression et de récession revêtent une grande importance pour l'évaluation des performances de l'irrigation par planches. Ces dernières années, les techniques d'analyse d'échelle ont permis de réduire les mesures requises et de formuler les relations sol–eau. Le but de cette étude était de développer une équation invariante pour le calcul des courbes de progression et de récession dans l'irrigation par planches à l'aide de techniques d'analyse d'échelle. Le modèle d'onde cinématique et l'équation d'infiltration de Philip ont été utilisés pour simuler l'irrigation par planches. Les facteurs d'échelle ont été définis de telle sorte que l'équation d'onde cinématique reste indépendante des conditions initiales et limites du sol. Les courbes de progression et de récession échelonnées montrent certains comportements, ce qui a conduit à introduire une équation de puissance et une équation binomiale pour les phases de progression et de récession, respectivement. Ces équations ont été appliquées sur 25 bordures végétalisées et non végétalisées. Quatre indices de performance ont été calculés pour chaque planche, notamment l'efficacité d'application (E_a), le rapport de percolation profonde (DPR), le rapport d'eau de queue (TWR) et l'efficacité des besoins en eau (E_r). Les résultats ont montré que la différence maximale entre les valeurs mesurées et estimées était de 4% pour E_a, 9% pour DPR et 4% pour E_r. Compte tenu de la simplicité et de l'indépendance des conditions de sols de la méthode proposée, on peut en conclure que les courbes de progression et de récession à l'échelle pourraient fournir une estimation raisonnable des performances de l'irrigation par planche. © 2019 John Wiley & Sons, Ltd.

MOTS CLÉS: irrigation par planche; infiltration; solution invariante; mise à l'échelle

*Correspondence to: Dr Mohammad Mahdi Chari, Unversity of Zabol, Water Engineering Department, Zabol +98543, Iran. E-mail: m.mahdi.chari@gmail.com
† Équation générale pour la progression et la récession de l'eau dans l'irrigation par planches.

INTRODUCTION

Surface irrigation is among the most common methods used for applying water on farms around the world, although water productivity is low in this type of irrigation (Adamala *et al.,* 2014). Surface irrigation systems can be assessed by their performance indices, such as advance and recession curves (Clemmens, 2007). There are three approaches for modelling the advance and recession phases in surface irrigation. The first is based upon hydraulic models (e.g. Sirmod, 2003; Bautista, 2012a), while the second approach deals with water balance models (e.g. for the advance phase: Strelkoff, 1977; Shepard *et al.,* 1993; Khatri and Smith, 2006; Ebrahimyan *et al.,* 2009, and for the recession phase: Strelkoff, 1977; Clemmens, 2007). The third refers to empirical models (e.g. for the advance phase: SCS method; and for the recession phase: Ram and Lal, 1971). Considering the application of Saint-Venant equations (continuity and momentum equations), there are the three approaches of the full hydrodynamic (HD), zero inertia (ZI) and kinematic wave (KW) models. All of these approaches should be solved by numerical methods and computer calculations. The water balance model, which is based on the continuity equation, is not capable of simulating some processes of surface irrigation such as recession phase and runoff volume. Empirical models have some coefficients which depend on input data and geometry of the borders. Based on the literature, one can see the importance of developing a hydraulic model that can accurately estimate advance and recession phases simultaneously.

In recent years, promising methods have been developed which reduce the requirements for measuring soil parameters such as infiltration (Khatri and Smith, 2006) and hydraulic conductivity (Kosugi and Hopmans, 1998). Miller and Miller (1956) were first to apply scaling techniques on soils based on the similar media concept (Miller and Miller, 1956; Sadeghi *et al.,* 2016). Based on this concept, however, two porous media are scaled through a physical characteristic length (scaling factor) when they are similar in their detailed microscopic geometry. Miller and Miller (1956) then suggested the concept of similar water flow in porous media in order to scale Darcy and continuity equations. They stated that water flow would be similar in two similar porous media and equal scaled initial and boundary conditions.

In general, porous media scaling has three different applications in soil physics: (i) studying the spatial variability of soil hydraulic functions (e.g. Warrick and Hussen, 1993; Sadeghi *et al.,* 2016); (ii) derivation of general solutions for soil water processes such as infiltration (Khatri and Smith, 2006; Sadeghi *et al.,* 2012); solute transport (Sadeghi and Jones, 2012) and soil moisture redistribution (Warrick and Hussen, 1993); (iii) formulation of soil water relations with minimum possible variables (e.g. Katopodes and Strelkoff, 1977; Yitayew and Fangemeier, 1984; Ram and Singh, 1985; Strelkoff and Clemmens, 1994; Alazba, 1999; Rasoulzadeh and Sepaskhah, 2003; Navabian *et al.,* 2009; Bautista *et al.,* 2012b).

In areas related to formulating equations of water and soil, governing equations of surface irrigation (e.g. Saint-Venant equations) are an example of scaling application. Based on Strelkoff and Clemmens (1981), transforming surface irrigation equations into dimensionless form, the number of independent parameters are reduced and, therefore, the general model is more understandable. Katopodes and Strelkoff (1977) and Strelkoff and Clemmens (1994) developed dimensionless (scaled) equations for border irrigation using reference variables (scaling factors). They also prepared graphs to use these equations based on soil types (e.g. α and k in the Kostiakov infiltration equation). However, a large number of graphs are required for all soil conditions. Yitayew and Fangemeier (1984) presented dimensionless graphs for open-ended border irrigation. The amount of runoff, then, could be calculated by having dimensionless length and cut-off time in the Kostiakov equation. Alazba (1999) plotted scaled advance curves of border irrigation corresponding to each number of infiltration families. As a result, water advance times can be acquired according to soil type and existing advance curves. Bautista *et al.* (2012b) improved the volume balance method by calculating water volume on the surface using a scaling technique.

In all the cases above, Saint-Venant equations were successfully scaled, while the results are not unique because of dependency on soil type. The infiltration equation changes from one soil to another, thus dimensionless equations of one soil cannot be used for others. Furthermore, the recession phase has not been discussed and formulated in the literature at all. However, SIRMOD (Walker, 2003) and SRFR/WinSRFR (Bautista *et al.,* 2012a) are the most comprehensive software developed so far for designing surface irrigation systems. But there are some instances where sufficient data are not available and use of a so-called quick method, that employs minimal measured data, is required. It is, therefore, important to develop, compare or evaluate these methods. Thus, the purpose of this study was to develop a quick method with a scaling approach for simulating the advance and recession phases in open border irrigation that is invariant to soil type, initial and boundary conditions.

MATERIALS AND METHODS

The two basic principles of conservation of mass and conservation of momentum, also known as the Saint-Venant equations, are fundamental to surface irrigation hydraulics (Strelkoff and Katopodes, 1977). Based on the Saint-Venant equations, different models have been developed to simulate water flow on the soil surface. While different models have used the mass conservation equation in the same way, application of the momentum conservation equation was different. In this concept, Saint-Venant equations are divided into three categories: full hydrodynamic, zero inertia and kinematic models. We used the kinematic wave model in this paper because of its simplicity.

Neglecting terms related to the dynamics of flow (i.e. longitudinal slope of field assumed equal to that of the energy grade line), the momentum equation can be solved using one of the steady-state equations which form the basis of stage–discharge relations (e.g. Manning, Chezy and Darcy–Weisbach equations). These models are known as steady depth or flow models. In the case of using the Manning equation, friction slope is $S_{\mathrm{f}} = S_0 = \frac{q^2 n^2}{y^{10/3}}$ (Walker and Humpherys, 1983), where n is roughness coefficient, q ($\mathrm{m}^2\ \mathrm{min}^{-1}$) is flow rate discharge per unit width, y (m) is flow depth, S_0 is longitudinal slope and S_{f} is friction slope.

The proper initial and boundary conditions (Equations (1a)–(1c))) are defined as

$$t = 0 : q(x, 0) = 0, y(x, 0) = 0 \tag{1a}$$

$$0 < t \leq t_{\mathrm{co}} : q(0, t) = q_0, y(0, x) = y_0 \tag{1b}$$

$$t > t_{\mathrm{co}} : q(0, t) = 0 \tag{1c}$$

where q_0 ($\mathrm{m}^2\ \mathrm{min}^{-1}$) is flow rate discharge per unit width, t_{co} (min) is time of cutoff and y_0 (m) is flow depth at the beginning of the border (normal depth).

Clemmens (1981) introduced a two-branch infiltration function and demonstrated its potential in modelling the infiltration process. This formulation is also used by WinSRFR 4.1 (Bautista *et al.,* 2012a). Since gravity force is negligible at the beginning of the border, the infiltration function may be read as $Z = St^{0.5}$ (Philip, 1957), where S ($\mathrm{mm/min}^{0.5}$) is sorptivity, t (min) is cumulative time and Z is infiltration depth (mm). As time continues, the infiltration rate approaches the final infiltration rate, and the equation becomes $Z = St_{\mathrm{b}}^{0.5} + f_0(t - t_{\mathrm{b}})$, where f_0 ($\mathrm{mm\ min}^{-1}$) is the final infiltration rate and t_{b} (min) is the branching time at the intersection of two branches; however, infiltration time and infiltration rate should be in conformity with each other. Thus, t_{b} is transition time from the first branch to the second:

$$t_{\mathrm{b}} = \left(\frac{0.5S}{f_0}\right)^2 \tag{2}$$

As a result, conservation equation for short and long times becomes:

$$\frac{\partial q}{\partial x} + \frac{\partial y}{\partial t} + 0.5St^{-0.5} = 0 \tag{3}$$

$$\frac{\partial \mathrm{q}}{\partial \mathrm{x}} + \frac{\partial \mathrm{y}}{\partial \mathrm{t}} + f_0 = 0 \tag{4}$$

Scaling

The first step in scaling any equation would be to transform parameters into dimensionless form by dividing them by a scaling factor. For the conservation and momentum equations (Equations (3) and (4)), dimensionless parameters are determined as follows:

$$\begin{aligned} q^* &= \frac{q}{q_c}, x^* = \frac{x}{X_c} \\ y^* &= \frac{y}{Y_c}, t^* = \frac{t}{T_c} \end{aligned} \tag{5}$$

where starred parameters are dimensionless parameters and q_c, Y_c, X_c and T_c are scaling factors for flow rate, flow depth, waterfront advance distance and time, respectively. The next step is to determine a few relations between scale factors and some physical parameters. Since the infiltration equation is different in the short and long term, scaling factors will also be different.

1 Short-term branch: Equation (5) is substituted into Equation (3), which results in

$$\frac{q_c}{X_c}\frac{\partial q^*}{\partial x^*} + \frac{Y_{\mathrm{c}}}{T_{\mathrm{c}}}\frac{\partial y^*}{\partial t^*} + 0.5ST_c^{-0.5}t^{*-0.5} = 0 \tag{6}$$

Equation (6) is made non-dimensional by dividing by $\frac{Y_c}{T_c}$:

$$\frac{q_c T_c}{X_c Y_c}\frac{\partial q^*}{\partial x^*} + \frac{\partial y^*}{\partial t^*} + 0.5\frac{ST_c^{0.5}}{Y_c}t^{*-0.5} = 0 \tag{7}$$

Scale factors are selected in such a way that the scaled kinematic wave equation will be independent of soil type and initial and boundary conditions. Since hydraulic parameters are time-independent at the beginning of the borders, scaling factors of flow rate (q_c) and flow depth (Y_c) are determined assuming a laminar flow at the beginning of the border. T_c and X_c are defined in such a way that the kinematic wave is independent of soil type. Thus, scaling factors are as follows:

$$q_{\mathrm{c}} = q_0 \tag{8}$$

$$Y_{\mathrm{c}} = \left(\frac{nq_0}{\sqrt{S_0}}\right)^{3/5} \tag{9}$$

$$T_c = 4\left(\frac{Y_c}{S}\right)^2 \tag{10}$$

$$X_c = \frac{q_C T_c}{Y_c} \tag{11}$$

Determining the scaling factors, the short-term scaled kinematic wave equation will become

$$\frac{\partial q^*}{\partial x^*} + \frac{\partial y^*}{\partial t^*} + t^{*-0.5} = 0 \tag{12a}$$

$$q^* = y^{*5/3} \tag{12b}$$

And scaled initial and boundary conditions will become

$$t^* = 0 : q^*(x^*, 0) = 0, y^*(x^*, 0) = 0 \tag{12c}$$

$$0 < t^* \leq t^*_{co} : q^*(0, t^*) = 1, y^*(0, t^*) = 1 \tag{12d}$$

$$t^* > t^*_{co} : q^*(0, t^*) = 0 \tag{12e}$$

2 Long-term branch: continuity Equation (4) in scaled form is as follows:

$$\frac{q_c T_{cl}}{X_{cl} Y_c}\frac{\partial q^*}{\partial x^*} + \frac{\partial y^*}{\partial t^*} + \frac{f_0 T_{cl}}{Y_c} = 0 \tag{13}$$

where scale factors of distance and time are determined by

$$T_{Cl} = \frac{Y_c}{f_0} \tag{14}$$

$$X_{cl} = \frac{q_C T_{cl}}{Y_c} \tag{15}$$

where q_c and Y_c are determined as described before. Having long-term scaled factors, the conservation equation becomes as follows, while the rest of equations are the same as Equations (12b)–(e):

$$\frac{\partial q^*}{\partial x^*} + \frac{\partial y^*}{\partial t^*} + 1 = 0 \tag{16}$$

Advance and recession curves are determined by putting initial and boundary conditions (Equations (12c)–(e)) into Equations (10)a and b and Equation (13).

Surface irrigation equations were solved numerically for short- and long-term branches, using Walker and Humpherys's (1983) approach. In this approach, a control volume is defined and water flow is divided into smaller squares of length δx. Inflow and outflow rates of each square as well as the cross section at the beginning and end of the border are different in each time step, δt (here 2 min). The cross section and advance distance (δx) of each time step are calculated using the Newton–Raphson method in Matlab software. Surface irrigation equations were solved for different sets of input parameters (i.e. flow rate, slope, border length, cutoff time and parameters of the Philip infiltration equation including S and f_0), and scaled curves were plotted for short- and long-term branches.

The uniqueness of the scaled solutions (Equations 12(a)–(e) and 16) also creates the possibility for the derivation of empirical models to approximate the advance and recession features by fitting to the scaled results. According to National Engineering Handbook (1974), a power advance function (Equation (17)) was fitted to long- and short-term scaled advance curves. A binomial equation (Equation (18)) was also fitted to long- and short-term scaled recession curves:

$$t^*_{Ax^*} = A_1 x^{*A_2} \tag{17}$$

$$t^*_{Rx^*} = B_1 x^{*2} + B_2 x^* \tag{18}$$

where $t^*_{Ax^*}$ and $t^*_{Rx^*}$ are advance and recession times of point x^* and A_1, A_2,$B_1$and B_2 are fitting parameters.

De-scaling

Parameters should be de-scaled to be useful in practical applications. De-scaled forms of Equations (17) and (18) are as follows:

$$t_x = a_1 x^{a_2} \tag{19}$$

$$t_x = b_1 x^2 + b_2 x \tag{20}$$

where

$$a_1 = \frac{T_c.A_1}{X_c^{A_2}}, a_2 = A_2 \tag{21}$$

$$a_1 = \frac{B_1 T_c}{X_c^2}, a_2 = \frac{B_2 T_c}{X_c} \tag{22}$$

Corresponding coefficients of each short- and long-term branch were used to de-scale the equations. Then, advance and recession curves were determined using input parameters of each border (parameters of flow and infiltration).

Model performance assessment

Typical assessment indices for surface irrigation systems consist of application efficiency (E_a), deep percolation ratio (DPR), tail water ratio (TWR) and water requirement efficiency (E_r). Results of the proposed model were compared with *in situ* measurements (or simulated with the zero-inertia model). Performance assessment indices can be defined as follows (Adamala *et al.,* 2014):

1 Full irrigation or over-irrigation situation:

$$E_a = \frac{Z_{req}L}{t_{co}q_0} \times 100 \tag{23}$$

$$\mathrm{DPR} = \frac{V_z - Z_{req}L}{t_{co}q_0} \times 100 \tag{24}$$

$$\mathrm{TWR} = 100 - E_a - \mathrm{DPR} \tag{25}$$

$$E_r = 100 \tag{26}$$

2 Deficit irrigation situation:

$$E_a = \frac{Z_{req}x_d + V_{zi}}{t_{co}q_0} \times 100 \tag{27}$$

$$\mathrm{DPR} = \frac{V_{za} - Z_{req}x_d}{t_{co}q_0} \times 100 \tag{28}$$

$$\mathrm{TWR} = 100 - E_a - \mathrm{DPR} \tag{29}$$

$$E_r = \frac{Z_{req}x_d + V_{zi}}{Z_{req}L} \times 100 \tag{30}$$

where Z_{req} (m) is the depth of water which was needed in the root zone, L (m) the total length of the border, V_z (m^2) the total volume of infiltrated water to the root zone per unit width, x_d (m) the length of the border where irrigation was sufficient and V_{zi} (m^2) the volume of water in insufficient irrigated area per unit width.

Data

Twenty-five data sets which were provided by Ram and Lal (1971), Ram and Singh (1985), Atchison (1973), and Roth (1974) were used to assess the application of the scaling method on border irrigation equations. Ram and Lal (1971) and Ram and Singh (1985) provided data of 18 closed-end borders, 9 of which were non-vegetated (R_j, $j = 1$, 2, ..., 9) and the others had wheat growing on them (R_j, j = 10, 11,..., 18). Atchison (1973) provided data of 6 open-ended borders of 5.98 m width, of which At-1, At-2, At-3, At-4 and At-5 had vegetation and At-17 was non-vegetation on the borders. Roth (1974) also provided one open-ended unplanted border (Roth-8). Parameters of the Philip (1957) equation (i.e. S and f_0) were determined using a two-point approach (Ebrahimian *et al.,* 2010). In order to improve the goodness of fit of the ordinary advance function (i.e. $x = pt^{0.5}$), the power was taken as unknown (i.e. $x = pt^r$).

Table I. Specifications of borders

Data set[a]	q_0 ($m^3m^{-1}m^{-1}$)	S_0 (m m^{-1})	n	Length (m)	S (mm $min^{-0.5}$)	f_0 (mm/ min)	t_b (min)
R-1	0.16	0.005	0.059	100	4.46	1.036	4.6
R-2	0.12	0.005	0.066	100	5.56	0.437	40.4
R-3	0.08	0.005	0.048	100	5.62	0.151	345.6
R-4	0.16	0.003	0.077	100	6.36	0.681	21.8
R-5	0.12	0.003	0.092	100	6.25	0.283	121.8
R-6	0.08	0.003	0.1	100	4.30	0.284	57.1
R-7	0.16	0.001	0.08	100	6.58	0.804	16.8
R-8	0.12	0.001	0.071	100	6.26	0.364	73.7
R-9	0.08	0.001	0.073	100	5.79	0.132	481.8
R-10	0.16	0.005	0.114	100	7.37	0.518	50.38
R-11	0.12	0.005	0.132	100	5.74	0.435	43.5
R-12	0.08	0.005	0.154	100	4.44	0.244	82.6
R-13	0.16	0.003	0.117	100	7.16	0.834	18.4
R-14	0.12	0.003	0.145	100	3.75	0.845	4.9
R-15	0.08	0.003	0.188	100	5.66	0.092	929.7
R-16	0.16	0.001	0.146	100	8.20	0.194	448.5
R-17	0.12	0.001	0.116	100	4.63	0.569	16.6
R-18	0.08	0.001	0.130	100	2.10	0.138	344.1
At-17	0.141	0.0011	0.06	91.4	4.05	0.363	36.3
At-1	0.141	0.0011	0.211	91.4	0.78	1.141	0.1
At-2	0.14	0.0011	0.107	91.4	1.74	1.012	0.7
At-3	0.113	0.0011	0.098	91.4	1.71	0.645	1.8
At-4	0.141	0.0011	0.119	91.4	0.611	0.132	0.1
At-5	0.085	0.0011	0.092	91.4	1.35	0.485	2.0
Roth-8	0.105	0.001	0.017	91.4	7.56	0.127	879.6

[a] R_j, j = 1, 2,..., 9 and R_j, j = 10, 11,..., 18: Ram and Lal (1971); Ram and Singh (1985).
At-17, At-1, At-2, At-3, At-4 and At-5: Atchison (1973).
Roth-8: Roth (1974).

Having the data of advance time and distance for two points along the border, one can determine the infiltration parameters (for more information about the two-point method, see Ebrahimian *et al.,* 2010). Specifications of borders are available in Table I.

RESULTS AND DISCUSSION

Scaling of advance and recession phases

Figure 1 shows the measured curves of the advance (Figure 1(a)) and recession (Figure 1(b)) phases for 25

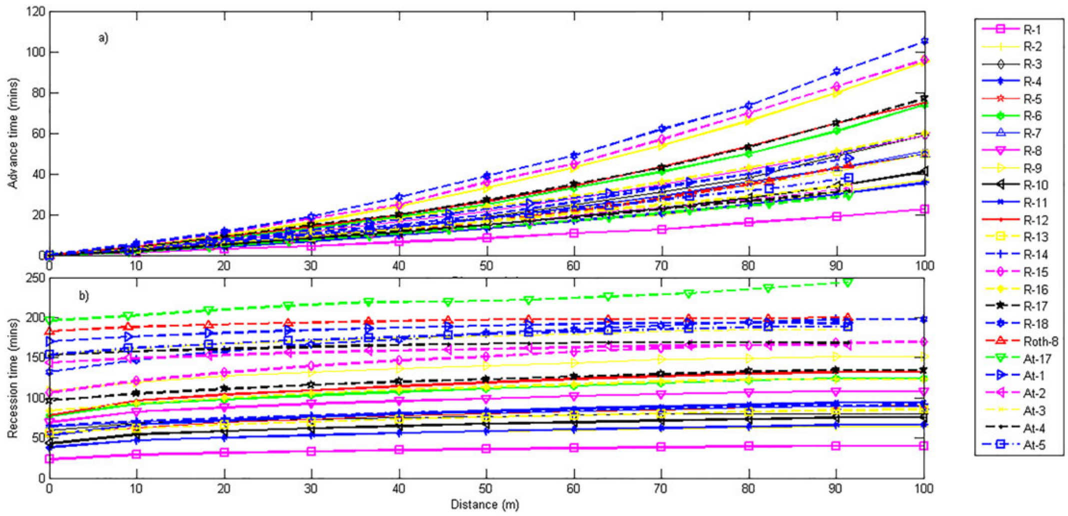

Figure 1. (a) Advance curves, and (b) recession curves of different borders [Colour figure can be viewed at wileyonlinelibrary.com]

Table II. Statistical indices of the scaling factors

Statistical indicators	q_c ($m^3\ m^{-1}\ min^{-1}$)	Y_c (m)	T_c (min)	X_c (m)	T_{cl} (min)	X_{cl} (m)	t_b (min)
Max.	0.16	0.080	42 900	85 900	426	826	929
Min.	0.08	0.015	16.4	113	25	107	0.704
Average	0.121	0.039	3 670	3 670	126	341	159
S.dv[a]	0.031	0.014	10 700	22 100	108	426	267
C.v[b]	0.16	0.368	2.9	2.8	0.86	0.62	1.67

[a]S.dv: Standard deviation.
[b]C.v: Coefficient of variation.

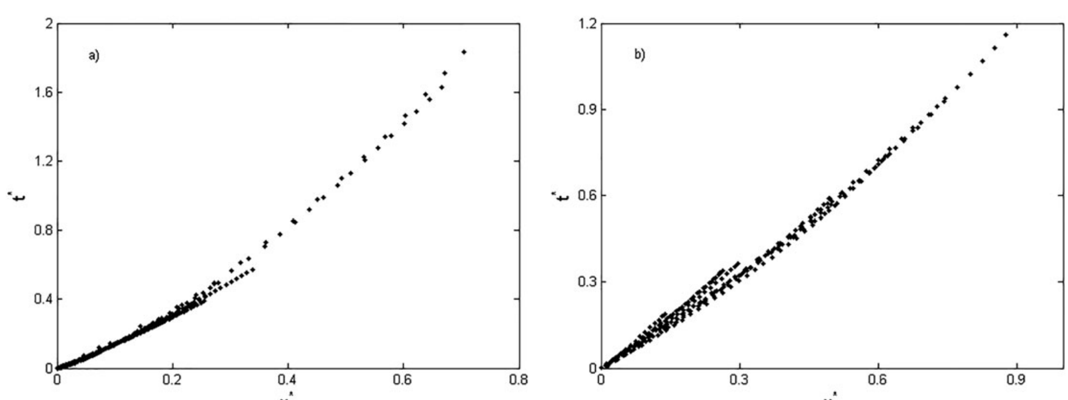

Figure 2. Scaled advance curves for (a) the short term and (b) the long term

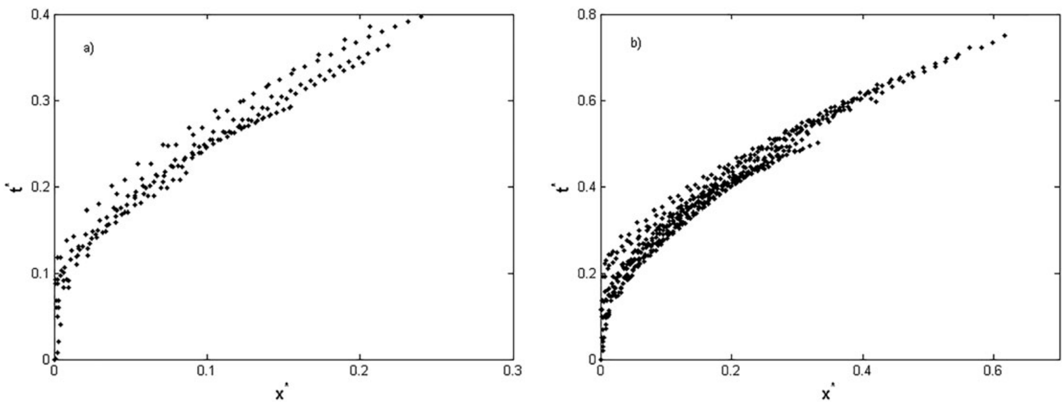

Figure 3. Scaled recession curves for (a) the short term and (b) the long term

borders in Table I. Figure 1 was plotted by considering measured data for advance phases and measured and zero-inertial estimated (for closed-end borders) data for recession phases for 25 borders. Based on Figure 1(a), R-1 and R-18 with 22.5 and 105 min had the shortest and the longest advance times, respectively, for 100-m borders. R-1 and At-17 with 40.3 and 244 min had the shortest and the longest advance times, respectively. The length of At-17 was 91.4 m. Different advance and recession times represent a pronounced variability in input flow parameters (boundary conditions) and infiltration parameters (soil type).

Each curve in Figure 1 was divided into long- and short-term sections using t_b from Table I. Then, the scaling factor of each curve was calculated using Equations (5), (10) and (11) for the short-term section, and Equations (5), (14) and (15) for the long-term section. Table II shows statistical indices, including minimum, maximum, mean, standard error and coefficient of variation for scaling factors and t_b. According to Equation (8), the amount of T_c has a positive correlation with normal depth (Y_c, which is dependent on S_0, n and q_0 according to Equation (9)), and a negative correlation with intake coefficient (S, which is related to soil texture and T_c). Roth-8 had the least T_c (16.4 min) which was in accordance with its small normal depth (0.015 m) and relatively large intake coefficient (0.00756 m/m$^{0.5}$). Based on Equation (11), there is a positive correlation between T_c and X_c which makes the parameters of T_c also effective on X_c. Regarding Table II, short-term curves have higher scaling factors ($16.4 < T_{cs} < 42\ 900$, and $113 < X_{cs} < 85\ 900$) than that of long-term curves ($24.7 < T_{cl} < 426$, and $107 < X_{cl} < 826$), which might be due to the narrower range of variation in the final infiltration rate (0.000092–0.001010 m min^{-1}) than in intake coefficient (0.000611–0.0082 m min$^{-0.5}$). In addition, the shape of the scaling equation of the short-term section (Equation (10)) is different from the long-term section. The amount of t_b was considerably different among the borders (ranging from 0.7 min for At-2 to 929 min for R-15), which shows its high variability in different soil textures.

Figures 2(a) and (b) show the scaled representation of Figure 1(a) for the short and long term, respectively. As can be seen, different scaling factors for the short and long term resulted in different counterpart figures. A scaled advance curve was plotted with respect to branching time (t_b^*) using the short-term advance curve (Figure 2(a)) for $t^* <= t_b^*$, and the long-term advance curve (Figure 3(b)) for $t^* > t_b^*$. It should be noted that scaled branching time (t_b^*) moves vertically in Figure 2 based on soil type (see Equations (2) and (5)). Figures 3(a) and (b) also show the scaled representation of Figure 1(b) for the short- and long term, respectively. Figures 2 and 3 show that each advance and recession curve (for both the short and long

Table III. Fitted parameters A_1, A_2, B_1 and B_2

	Timescale	Coefficients
Advance	Short	$A_1 = 4.02, A_2 = 1.46$
	Long	$A_1 = 1.41, A_2 = 1.13$
Recession	Short	$B_1 = -3.15, B_2 = 2.82$
	Long	$B_1 = -8.77, B_2 = 3.21$

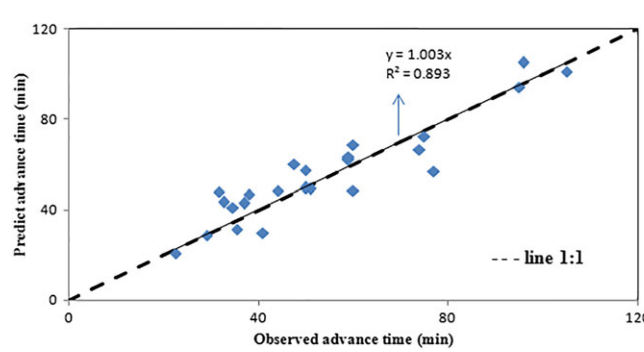

Figure 4. Comparison between observed and predict advance times [Colour figure can be viewed at wileyonlinelibrary.com]

term) approach a certain equation, and scaling factors can be suitably determined and the scaling method was successful in modelling the advance phase in border irrigation.

General advance and recession equation

Equations (17) and (18) were fitted to scaled advance (Figures 2(a) and (b)) and recession (Figures 3(a) and (b)) curves, respectively. Results were significant at a level of 1% and are provided in Table III. De-scaled advance and recession curves were obtained using Equations (19) and (20), coefficients in Table III and input data of each border.

Advance phase

In order to evaluate the scaling results, estimated advance times (time to reach the end of the border) were plotted against measured values (Figure 4). Comparing the scattered points with the 1 : 1 line shows the accuracy of the scaling method in modelling the advance phase of border irrigation.

Katopodes and Strelkoff (1977) plotted the advance curves corresponding to different α values (from 0.1 to 0.9) using the zero-inertia model, where α is the power of the Kostiakov infiltration function. Having input parameters, including flow rate, slope, roughness and parameters of the Kostiakov infiltration function, one can determine the scaling factors of a border and as a result determine the scaled

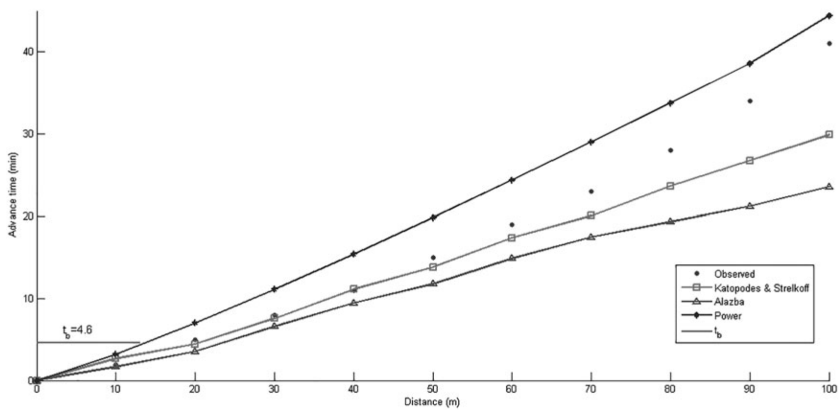

Figure 5. Advance curve in border R-10 using observed data, Alazba, Katopodes and Strelkoff and power models [Colour figure can be viewed at wileyonlinelibrary.com]

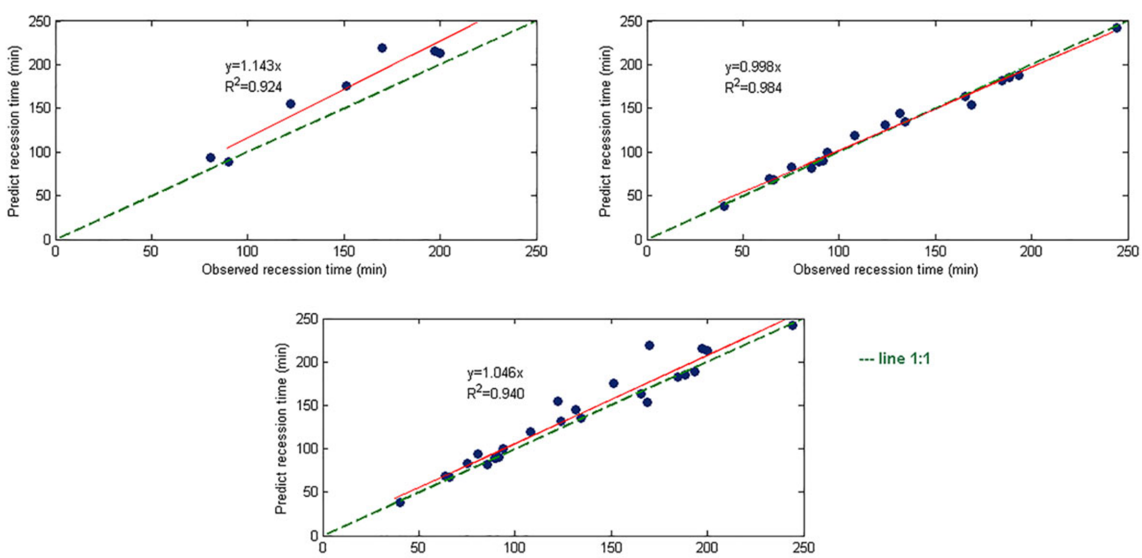

Figure 6. Comparison of observed and estimated recession times for (a) short term and (b) long term and (c) overall sections [Colour figure can be viewed at wileyonlinelibrary.com]

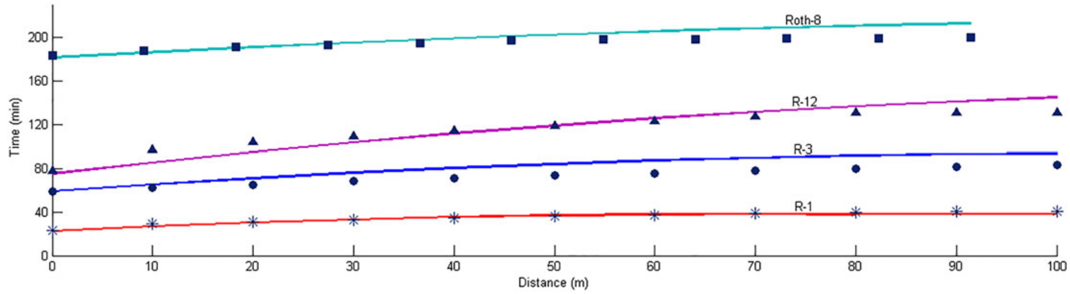

Figure 7. Observed and estimated recession curves for borders R-1, R-3, R-12 and Roth-8 (dots are observed and line is modelled recession) [Colour figure can be viewed at wileyonlinelibrary.com]

advance curve. For a different α-value from those mentioned before (i.e. 0.1–0.9), the scaled advanced curve can be estimated by interpolating the available curves. Alazba (1999) obtained scaled advance curves of 14 infiltration curve numbers which covers most soil types (i.e. from 0.1 to 4), using a scaled form of the volumetric water balance equation (Hart model). A corresponding set of parameters of the Kostiakov equation to each infiltration curve number were determined and the advance curve was calculated from that. As with Katopodes and Strelkoff (1977), Alazba (1999) estimated the advance curves of different α-values by interpolating the available curves. Figure 5 shows measured and estimated advance curves using the power model, and Alazba (1999) and Katopodes and Strelkoff (1977) models for R-10. Alazba, power and Katopodes and Strelkoff models had progressively better results because of using the Hart water balance equation, kinematic wave model and zero-inertia model, respectively. In Figure 6, however, we had weaker results by obtaining distance from the beginning of the border in the Alazba and Katopodes and Strelkoff models. α-value of border R-10 was 0.35, and was not available in scaled graphs. Therefore, the advance curve of this border was estimated by interpolation and of course might introduce some errors. Calculated scaled factors of time (min) and length (m) for border R-10 were $T_c = 446.1$, $X_c = 1917.5$ using the Katopodes and Strelkoff model, and $T_c = 235.7$, $X_c = 1266.9$ using the Alazba model. Since calculated scaling factors are relatively high, a small error in calculations or interpolations can cause a big error in real conditions due to multiplication of the scale factor by a dimensionless value. It may be concluded that the proposed equation in this paper is superior to other methods of estimating advance curves due to its simple form, having the accuracy of the kinematic wave model, and finally eliminating the need for graphical interpolation.

Recession phase

Measured recession times (or estimated by the zero-inertia model for closed-ended borders) were plotted against estimated recession times (using Equation (20)) for 25 borders whose specifications are provided in Table I for the short term (borders R-3, R-5, R-9, R-15, R-16, R-18 and Roth-8), long term and total borders (Figure 6). As can be seen in Figure 7, the proposed equation for the long-term branch had better results in modelling the recession phase in comparison with the short-term equation, which may be due to using a linear infiltration function ($Z = St_b^{0.5} + f_0(t - t_b)$) for the long-term branch. Clemmens (1981) also

Table IV. Irrigation efficiencies on the basis of calculated and observed advance and recession time (min) for depth of water need in root zone 0.1 m

Data set	Observed				Predicted			
	E_a	DPR	TWR	E_r	E_a	DPR	TWR	E_r
R-1	86.3	0	13.7	31.1	83.1	0	16.9	29.9
R-2	79.8	0	20.2	35.5	77.7	0	22.2	34.5
R-3	84.9	0	15.1	40.1	87.9	0	12.1	41.5
R-4	76.2	0	23.8	43.3	75.5	0	24.4	42.9
R-5	78.2	0	21.8	46.9	76.4	0	23.6	45.8
R-6	65.5	0	34.9	38.5	66.2	0	33.8	39.2
R-7	76.2	0	23.8	61.0	73.2	0	26.8	58.5
R-8	74.6	0	25.4	52.8	72.7	0	27.3	51.5
R-9	75.1	0	24.9	57.1	77.6	0	22.3	59.1
R-10	77.7	0	22.3	50.1	80.2	0	19.7	52.6
R-11	73.2	0	26.8	44.8	72.3	0	27.7	44.5
R-12	67.5	0	32.5	40.5	68.4	0	31.6	41.1
R-13	75.2	0	24.8	60.1	76.1	0	23.9	60.8
R-14	80.0	0	20.0	57.6	76.6	0	23.4	54.7
R-15	75.9	0	24.1	58.3	78.1	0	21.9	60.0
R-16	78.2	0	21.8	75.1	76.1	0	23.9	73.3
R-17	65.1	0	34.9	60.2	65.2	0	34.8	60.2
R-18	69.2	0	30.7	58.2	67.1	0	32.9	56.3
At-17	27.8	0	72.1	81.7	27.9	0	72.1	81.6
At-1	44.1	38.7	17.2	100	44.1	29.7	26.2	100
At-2	50.2	22.9	26.9	100	50.2	18.6	31.2	100
At-3	57.4	1.8	40.8	99.8	56.5	0.4	43.0	97.8
At-4	46.0	43	11.0	100	47.8	40.0	12.2	100
At-5	59.8	0	40.1	77.8	56.7	0	43.3	73.7
Roth-8	47.3	52.1	0.6	98.7	47.7	51.8	0.50	99.6

used a branching approach for evaluating border irrigation systems and reported similar results. Based on the literature (Ram and Lal, 1971; Strelkoff, 1977), the flow regime of the recession phase is generally laminar or transition, which makes the use of linear infiltration functions more logical.

In order to visualize the results, recession curves of a few borders were plotted in Figure 7, representing short-term borders (R-3 and Roth-8) and long-term borders (R-1 and R-12). Figure 7 shows the relative success of the scaling approach (Equation (20)) in modelling recession curves of open-ended recession curves.

Performance assessment of the proposed method

Performance indices (application efficiency (E_a), deep percolation ratio (DPR), tail water ratio (TWR) and water requirement (storage) efficiency (E_r)) for a 0.1 m irrigation depth of measured (or estimated by the zero-inertia model) and modelled by the proposed scaling method are provided in Table IV. According to Table IV, the maximum difference between measured and estimated E_a, DPR and E_r was 4, 9 and 4% in R-14, At-1 and At-5, respectively. Based on the results, it can be concluded that the proposed relations had a good performance in modelling the advance and recession phases of border irrigation.

[Table IV. Irrigation efficiencies on the basis of calculated and observed advance and recession times (min) for depth of water need in root zoon 0.1 m.]

Effects of vegetation cover on advance and recession equations

Figure 8 shows the observed and predicted advance (a) and recession (b) times as calculated by Equations (19) and (20)

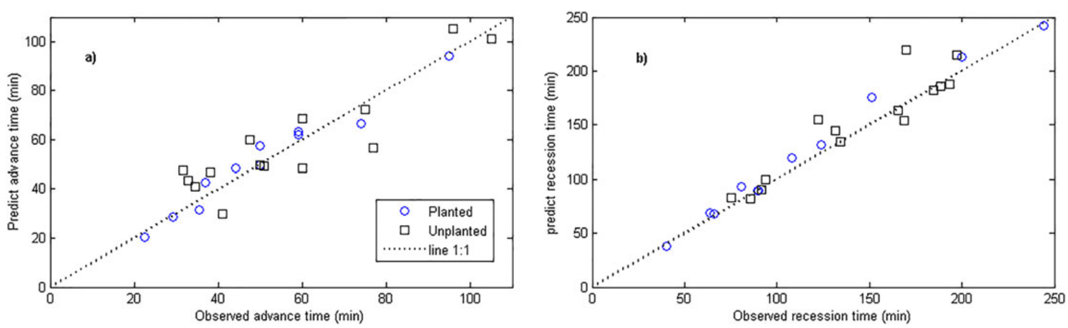

Figure 8. Comparison of observed and predicted (a) advance times and (b) recession times for planted and unplanted borders [Colour figure can be viewed at wileyonlinelibrary.com]

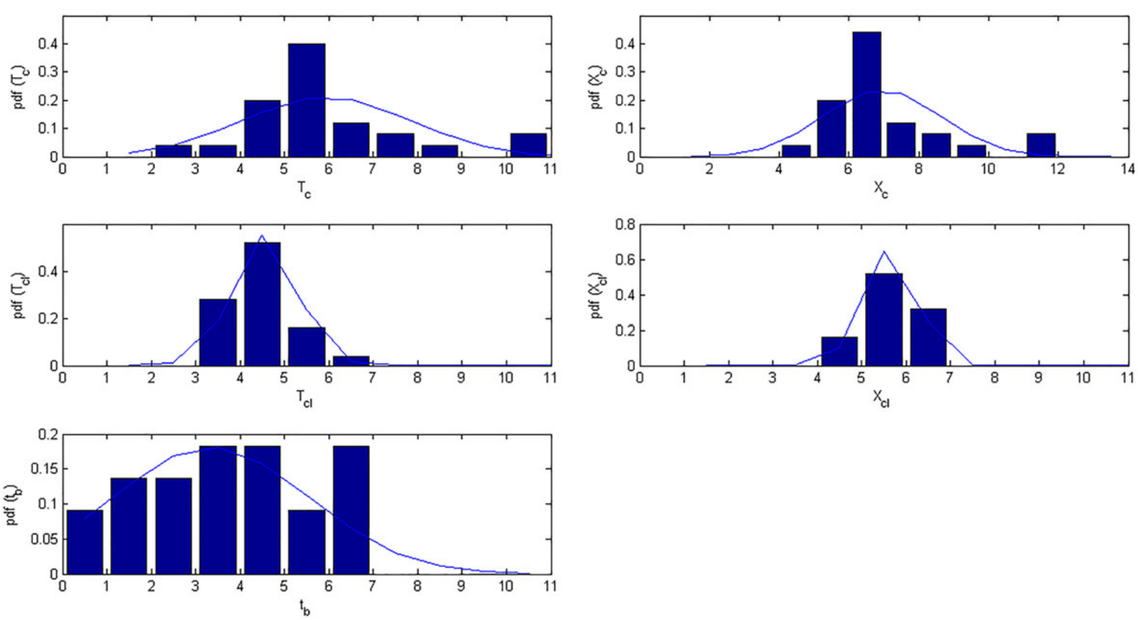

Figure 9. Frequency distribution of scaling factors and t_b as measured (bar chart) and lognormal-calculated (line chart) for the short and long term [Colour figure can be viewed at wileyonlinelibrary.com]

for non-vegetated and vegetated borders. Mean absolute errors ($\left|\frac{Observed-predicted}{Observed}\right|\times 100$) of advance times in non-vegetated and vegetated borders were 7.8 and 18.4%, respectively. These values in the recession phase were 6.78 and 8.08% for unplanted and planted borders, respectively. Results show that advance and recession equations have better estimates in non-vegetated borders, although in general one can say that soil type and vegetation cover did not have a significant impact on the results and the power function was valid in most irrigation conditions.

The probability density functions (pdf) of scaling factors

The probability density functions (pdfs) of space and time scaling factors were also evaluated. Figure 9 shows the frequencies of measured (bar chart) and lognormal estimated (line chart) scale factors for two short and long terms as well as t_b. As can be seen in Figure 9, space and time scaling factors have a similar shape for both the short and long term and follow a lognormal distribution. There are no previous studies on the probability distribution of scale factors of surface irrigation, but lognormal distribution functions are reported for scale factors for soil hydraulic parameters (Kosugi and Hopmans, 1998).

CONCLUSION

Previous studies on scaling the advance phase of surface irrigation were dependent on soil type and were in graphical form (Katopodes and Strelkoff, 1977; Yitayew and Fangemeier, 1984; Strelkoff and Clemmens, 1994; Alazba, 1999). The proposed method in this study consisted of using a scaling method and the Philip infiltration step function in a way that eliminates graphical interpolations and soil type dependencies. Since the recession phase of border irrigation is of great importance and equations that model this phase are very limited, a new method for estimating the recession curve of open-ended borders was introduced based on the scaling method. Advance and recession curves of short and long term were determined using space and time scaling factors. Space and time scaling factors followed a lognormal distribution function in both the short and long term, in accordance with other scale factors in soil physics. Simple shape and independence from soil type are among the advantages of using the proposed functions. Application results of the proposed method on 25 vegetated and non-vegetated borders were evaluated by performance indices, including application efficiency (E_a), deep percolation ratio (DPR), tail water ratio (TWR) and water requirement efficiency (E_r). The results of the evaluations showed the accuracy of the proposed equations by the scaling method. Except for restrictions on the use of the kinematic wave model, it can be concluded that the proposed method can be used in all other cases and makes computations easier and shorter in the process of evaluation of border irrigation.

REFERENCES

Adamala S, Raghuwanshi NS, Mishra A. 2014. Development of Surface Irrigation Systems Design and Evaluation Software (SIDES). *Computers and Electronics in Agriculture* **100**: 100–109.

Alazba AA. 1999. Dimensionless advance curves for infiltration families. *Agricultural Water Management* **41**: 115–131.

Atchison KT. 1973. *Retragance coefficient and other data for a vegetated irrigation border*. Unpublished MS thesis, University of Arizona: Tucson, USA.

Bautista E, Schlegel J, Strelkoff TS. 2012a. *WinSRFR 4.1, Software and User Manual USDA-ARS* U.S. Arid Land Agricultural Research Center Maricopa: Ariz, USA.

Bautista E, Strelkoff T, Clemmens AJ. 2012b. Improved surface volume estimates for surface irrigation volume-balance calculations. *Journal of Irrigation and Drainage Engineering ASCE* **138**: 715–726.

Clemmens AJ. 1981. Evaluation of infiltration measurements for border irrigation. *Agricultural Water Management* **3**: 251–267.

Clemmens AJ. 2007. Simple approach to surface irrigation design: theory. *Journal of Land and Water* **1**: 1–19.

Ebrahimian H, Liaghat A, Ghanbarian-Alavijeh B, Abbasi F. 2010. Evaluation of various quick methods for estimating furrow and border infiltration parameters. *Irrigation Science* **28**(6): 479–488.

Katopodes ND, Strelkoff T. 1977. Dimensionless solutions of border irrigation advance. *Journal of Irrigation and Drainage Engineering ASCE* **103**(4): 401–417.

Khatri KL, Smith RJ. 2006. Real-time prediction of soil infiltration characteristics for the management of furrow irrigation. *Irrigation Science* **25**(1): 33–43.

Kosugi K, Hopmans JW. 1998. Scaling water retention curves for soils with lognormal pore-size distribution. *Soil Science Society of America Journal* **62**: 1496–1504.

Miller EE, Miller RD. 1956. Physical theory for capillary flow phenomena. *Journal of Applied Physics* **27**: 324–332.

National Engineering Handbook. 1974. *Border irrigation*. US Soil Conservation Service (SCS): Washington, DC; ch. 4.

Navabian M, Liaghat AM, Smith RJ, Abbasi F. 2009. Empirical functions for dependent variables in cutback furrow irrigation. *Irrigation Science* **27**: 215–222.

Philip JR. 1957. The theory of infiltration—3: moisture profiles and relation to experiment. *Soil Science* **84**: 163–178.

Ram RS, Lal R. 1971. Recession flow in border irrigation. *Journal Agricultural Engineering India* **8**(3): 62–70.

Ram RS, Singh VP. 1985. Application of kinematic wave equations to border irrigation design. *Journal of Agricultural Engineering Research* **32**: 57–71.

Rasoulzadeh A, Sepaskhah AR. 2003. Scaled infiltration equations for furrow irrigation. *Biosystems Engineering* **86**(3): 375–383.

Roth RL. 1974. Data for border irrigation models. *Transactions of ASAE* **17**(1): 157–161.

Sadeghi M, Jones SB. 2012. Scaled solutions to coupled soil-water flow and solute transport during the redistribution process. *Vadose Zone Journal* **11**(4): vzj2012.0023. https://doi.org/10.2136/vzj2012.0023.

Sadeghi M, Ghahraman B, Ziaei AN, Davary K, Reichardt K. 2012. Additional scaled solutions to Richards' equation for infiltration and drainage. *Soil and Tillage Research* **119**: 60–69.

Sadeghi M, Ghahraman B, Warrick AW, Tuller M, Jones SB. 2016. A critical evaluation of the Miller and Miller similar media theory for application to natural soils. *Water Resources Research* **52**(4): 1–18.
Shepard JS, Wallender WW, Hopmans JW. 1993. One method for estimating furrow infiltration. *Transactions of ASAE* **36**(2): 395–404.
Strelkoff T. 1977. Algebraic computation of flow in border irrigation. *Journal of Irrigation and Drainage Engineering ASCE* **103**: 357–377.
Strelkoff T, Katopodes ND. 1977. Border irrigation hydraulics with zero inertia. *Journal of Irrigation and Drainage Engineering ASCE* **103**(3): 325–342.
Strelkoff T, Clemmens AJ. 1981. Dimensionless stream advance in sloping borders. *Journal of Irrigation and Drainage Engineering ASCE* **107**(4): 361–382.
Strelkoff T, Clemmens AJ. 1994. Dimensional analysis in surface irrigation. *Irrigation Science* **15**(2–3): 57–82.
Walker WR. 2003. *SIRMOD III: surface irrigation simulation, evaluation and design. Guide and technical documentation*. Dept. of Biological and Irrigation Engineering. Utah State Univ: Logan, Utah, USA.
Walker WR, Humpherys AS. 1983. Kinematic-wave furrow irrigation model. *Journal of Irrigation and Drainage Engineering ASCE* **109**(1R4): 377–392.
Warrick AW, Hussen AA. 1993. Scaling of Richards' equation for infiltration and drainage. *Soil Science Society of America Journal* **57**: 15–18.
Yitayew M, Fangemeier DD. 1984. Dimensionless runoff curves for irrigation borders. *Journal of Irrigation and Drainage Engineering ASCE* **110**: 179–191.

